

# Nondestructive Replication of Self-Ordered Nanoporous Alumina Membranes via Cross-Linked Polyacrylate Nanofiber Arrays

Silko Grimm,<sup>†</sup> Reiner Giesa,<sup>‡</sup> Kornelia Sklarek,<sup>†</sup> Andreas Langner,<sup>†</sup>  
Ulrich Gösele,<sup>†</sup> Hans-Werner Schmidt,<sup>‡</sup> and Martin Steinhart<sup>\*†</sup>

*Max Planck Institute of Microstructure Physics, Weinberg 2, D-06120 Halle, Germany, and Macromolecular Chemistry I and Bayreuth Institute for Macromolecular Research (BIMF), University of Bayreuth, D-95440 Bayreuth, Germany*

Received March 24, 2008; Revised Manuscript Received May 5, 2008

## ABSTRACT

Ordered nanofiber arrays are a promising material platform for artificial adhesive structures, tissue engineering, wound dressing, sensor arrays, and self-cleaning surfaces. Their production via self-ordered porous alumina hard templates serving as shape-defining molds is well-established. However, their release requires the destruction of the hard templates, the fabrication of which is costly and time-consuming, by wet-chemical etching steps with acids or bases. We report the nondestructive mechanical extraction of arrays of cross-linked polyacrylate nanofibers from thus recyclable self-ordered nanoporous alumina hard templates. Silica replicas of the latter were synthesized using the extricated nanofiber arrays as secondary molds that could be mechanically detached from the molded material. The approach reported here, which can be combined with microstructuring, may pave the way for the high-throughput production of both functional nanofiber arrays and ordered nanoporous membranes consisting of a broad range of material systems.

Shape-defining hard templates containing arrays of aligned cylindrical nanopores allow the formation of a plethora of materials into nanofibers.<sup>1–5</sup> Self-ordered porous alumina<sup>6–10</sup> (anodic aluminum oxide, AAO) is a particularly attractive mold that is characterized by regularly arranged, parallel pores with narrow diameter distribution and uniform pore depth arranged in a hexagonal lattice consisting of grains extending 10–20 lattice periods. It is readily available and is routinely produced with lattice constants ranging from 65 to 500 nm, pore diameters ranging from 25 to 400 nm, and pore depths adjustable to values between a few 100 nm and several 100  $\mu\text{m}$ . Arrays of freestanding polymeric nanofibers derived from parent AAO hard templates are being considered as a potential material platform for sensor arrays, bioinspired artificial adhesive structures,<sup>11–13</sup> wound dressing, and tissue engineering.<sup>14,15</sup> Moreover, they may serve as surfaces exhibiting specific wetting properties<sup>16–18</sup> or self-cleaning behavior.<sup>19</sup> Nanofiber arrays have been used as secondary molds for the replication of their parent AAO hard templates serving as primary molds.<sup>20–22</sup> Drawbacks associated with the generation of nanopore arrays by combining block copolymer lithography and reactive ion etching,<sup>23</sup> such

as tapered pore profiles,<sup>24</sup> polymerization of the etchant on the pore walls, poor etch contrast, and underetching,<sup>25</sup> can thus be circumvented. However, the release of the nanofiber arrays after the primary molding step requires the destruction of the parent AAO hard templates by wet-chemical etching with bases or acids.<sup>20–22</sup> Despite the fact that the preparation of the primary molds is the most costly and time-consuming step in the entire process chain, it is, therefore, impossible to obtain multiple replicas from a master template. The destruction of the parent AAO hard templates, so far inevitable, is a general drawback of scaling-up template-based approaches to the production of nanofiber arrays.

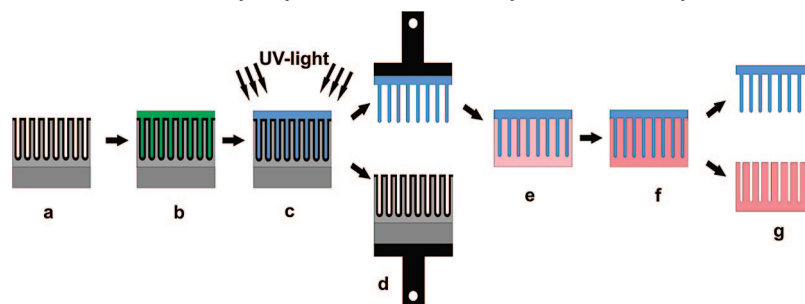
Here, we report the nondestructive mechanical extraction of arrays of nanofibers consisting of cross-linked polyacrylate networks from thus recyclable self-ordered AAO hard templates with a pore diameter of 120 nm, which avoids the drawbacks of the template-based replication processes discussed above. The nanofiber arrays obtained have been used as secondary molds for the fabrication of silica replicas of the AAO primary molds by means of sol/gel chemistry. The silica replicas also contain ordered arrays of aligned nanopores. It is straightforward that alternative synthesis methods such as electrodeposition<sup>20,26</sup> or atomic layer deposition<sup>27</sup> can also be applied and that, for example, nanoparticles, dyes,

\* Corresponding author. E-mail: steinhart@mpi-halle.de.

<sup>†</sup> Max Planck Institute of Microstructure Physics.

<sup>‡</sup> University of Bayreuth.

**Scheme 1.** Schematic Diagram of the Nondestructive Replication of Self-Ordered AAO Based on the Use of Cross-Linked Polyacrylate Nanofiber Arrays As Secondary Molds<sup>a</sup>



<sup>a</sup> The parent AAO hard template (grey), which is attached to an underlying aluminum substrate (dark grey), is coated with a multilayer of a perfluorated silane coupling agent (black) to reduce the surface energy of the pore walls (panel a). Resin (green) is infiltrated into the nanopores by a pressure impregnation technique (panel b) and photo-cross-linked (panel c). The obtained array of cross-linked polyacrylate nanofibers (blue) is extracted from the parent AAO hard template by mechanical extraction (panel d). Whereas the AAO can be reused, the nanofiber array is covered with a sol/gel (light pink) (panel e), which is gelled (panel f). Finally, the nanofiber array is mechanically detached from the gelled replica (pink) of the parent AAO hard template (panel g).

or even biomolecules can be incorporated into the nanoporous replicas. Their nondestructive detachment from recyclable AAO primary molds may pave the way for the mass production of nanofiber arrays. Using the nanofiber arrays as likewise recyclable secondary molds may enable nondestructive high-throughput copying of the parent AAO hard templates with a broad range of materials.

In general, extractions were accomplished by the application of a force parallel to the pore axes of the hard templates. However, slight misalignment, which could not be avoided when the samples were mounted for the extraction experiments, resulted in shear forces perpendicular to the pore axes and hence in lateral displacement. Previous attempts to detach mesoporous silica microrods from macroporous silicon hard templates<sup>28</sup> with pore diameters in the micrometer range were facilitated by their pronounced shrinkage during high-temperature calcination.<sup>29</sup> However, the macroporous silicon could only be recovered by a tedious procedure which involved etching of the silica layer covering the pore walls and residual segments of the mesoporous microrods still located inside the pores with an aqueous HF solution, treatment with a boiling H<sub>2</sub>SO<sub>4</sub>/H<sub>2</sub>O<sub>2</sub> mixture, and modification with 1H,1H,2H,2H-perfluorodecyltrichlorosilane, resulting in an increase of the pore diameter by about 30 nm per recovery cycle. The extraction of microrods consisting of thermoplastics such as polystyrene or polyvinylidene fluoride from macroporous silicon hard templates suffered from plastic deformation.<sup>30</sup> Microrods jammed in the pores were prone to yielding and necking, leading to elongation along with a decrease in their cross-sectional area, that is, their diameter, and eventually to fracture (Supporting Information, Figure S1).

The extraction of nanofiber arrays from AAO hard templates with pore diameters in the 100 nm range is associated with even larger contact areas and lower shear tolerance. It is reasonable to assume that nanofibers exhibiting a network structure accompanied by elasticity at small deformations could be drawn out of the nanopores without formation of structural defects or fracture. Materials such as cross-linked polymers forming three-dimensional networks are capable of dissipating energy without irreversible plastic deformation, whereas materials such as thermoplastics tend

to irreversibly deform or fracture upon exposure to shear forces. Three-dimensional networks of cross-linked polymers do not show yielding or necking and exhibit excellent resistance to heat, solvents, and other chemicals. A wide variety of cross-linkable systems is commercially available, including heat setting systems such as epoxy resins, or photo-cross-linkable systems such as polyacrylates. Radiation curing with UV light is a fast, emission-free process characterized by high penetration depths which can be performed under ambient conditions. For the preparation of the nanofibers, we therefore used BASF Laromer radiation curing resins, for which many formulations differing in monomer chemistry, reactivity, viscosity, and stiffness of the cured material are available. The properties of the resins used in this work are summarized in Table S1 (Supporting Information).

Self-ordered AAO hard templates<sup>8</sup> (the nanoporous AAO layers were attached to underlying aluminum substrates so that the pore bottoms were closed) with an initial pore diameter of 200 nm were coated with 1H,1H,2H,2H-perfluorodecyltrichlorosilane<sup>31</sup> to minimize adhesion between the pore walls and the nanofibers formed inside the nanopores. Homocondensation led to the formation of an approximately 40 nm thick multilayer of the polymerized silane coupling agent, as determined by scanning electron microscopy (SEM),<sup>32</sup> thus reducing the pore diameter of the AAO hard templates to about 120 nm (Scheme 1, panel a). A mixture of PO 77F, an amine-modified oligoetheracrylate resin, and 4 wt % of a free-radical photoinitiator (Irgacure 651)<sup>33</sup> was injected into the AAO hard templates at room temperature by applying a pressure impregnation technique<sup>34</sup> (Scheme 1, panel b) because the low surface energy of the silanized pore walls prevented spontaneous infiltration of the PO 77F resin. Photopolymerization by exposure to UV light generated by a Fusion UV Curing F300 lamp (D lamp; 120 W/cm) for 1 s resulted in the formation of nanofibers consisting of cross-linked polyacrylate inside the nanopores that were connected with a cross-linked polyacrylate film on top of the AAO hard template (Scheme 1, panel c). Studs were glued to the upper polymeric surface and the underside of the aluminum substrate, and the nanofibers were removed from the AAO hard template using a linear motion device

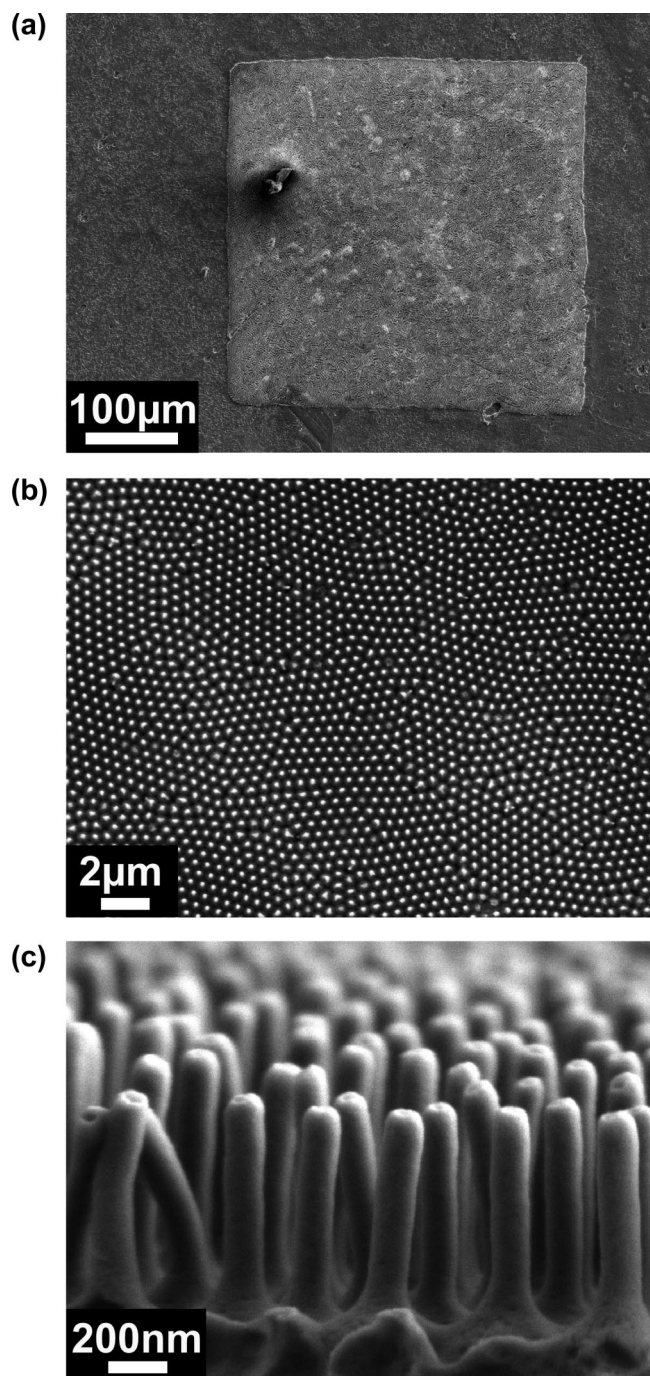


**Figure 1.** Scanning electron microscopy (SEM) images of detached arrays of polyacrylate nanofibers (diameter  $\approx 120$  nm; length  $\approx 900$  nm) and their parent AAO hard templates. Images a–c show nanofiber arrays with a side length of about  $500 \mu\text{m}$ . (a) Large field view; (b) top view, evidencing that the nanofiber array exhibits the characteristic domain structure of the parent AAO hard template; (c) side view of the nanofiber array.

with an attached load cell. First, a piston with adhesive tape was pressed onto the sample at a rate of  $0.2 \text{ mm/min}$  with a maximum compressive load of  $-40 \text{ N}$ . Then, the nanofibers were lifted at a rate of  $0.1 \text{ mm/min}$  with a force of around  $0.4 \text{ N}$  (Scheme 1, panel d). To synthesize silica replicas of the parent AAO hard templates, a sol solution containing tetraethyl orthosilicate (TEOS; Alfa Aesar), deionized  $\text{H}_2\text{O}$ , 37% HCl, and absolute ethanol at a molar ratio of 1:6:0.001:

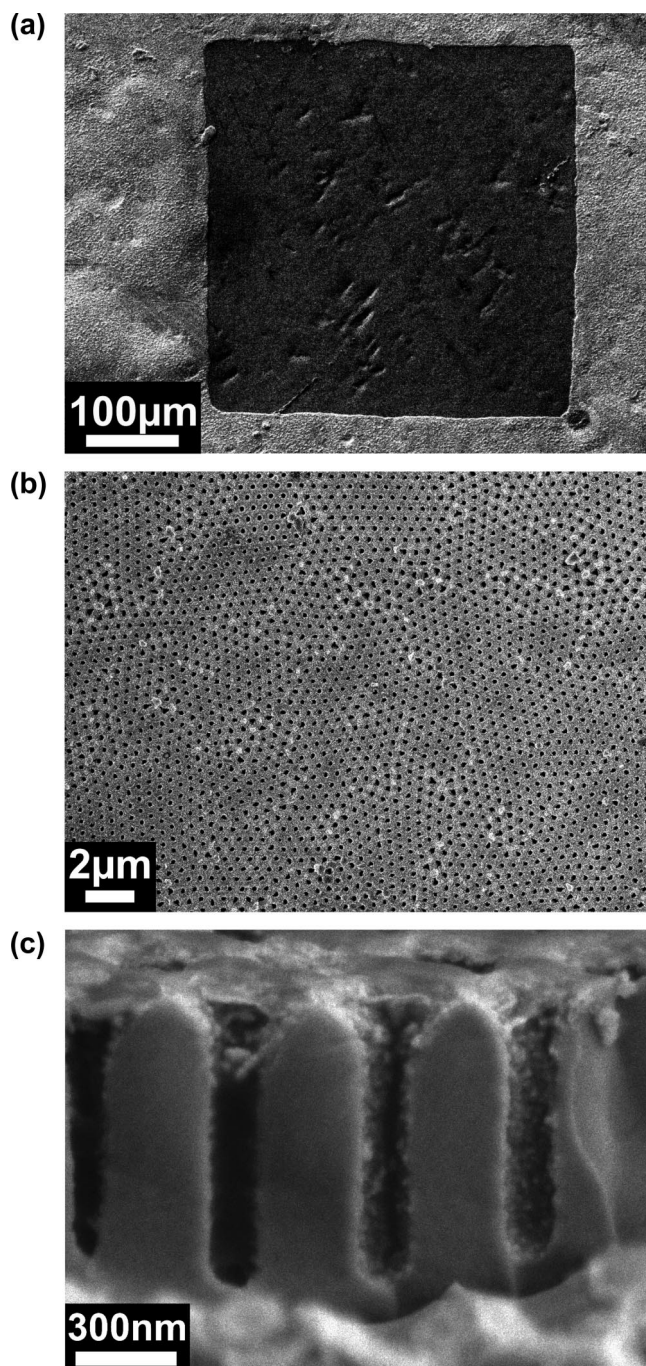


**Figure 2.** SEM images a–c show the parent AAO hard template after the mechanical extraction of the nanofibers seen in Figure 1. (a) Large-field view. The nanofibers were extracted from the darker square in the center; the nanopores in the surrounding bright rim were sealed with a gold layer (see main text for details). (b) Pore openings after extraction in the central square at higher magnification. (c) Cross-sectional view of nanopores located in the central square which have walls covered with a  $40 \text{ nm}$  thick silane layer after extraction of the nanofibers.

8.8 was stirred for 3 h. Then the polyacrylate nanofiber arrays serving as secondary molds were placed at the bottom of a reaction tube and covered with the sol solution (Scheme 1, panel e). After gelation at room temperature for 48 h and at  $60^\circ\text{C}$  for 24 h (Scheme 1, panel f), the polyacrylate nanofiber arrays could be easily detached from the nanoporous silica films with tweezers (Scheme 1, panel g).

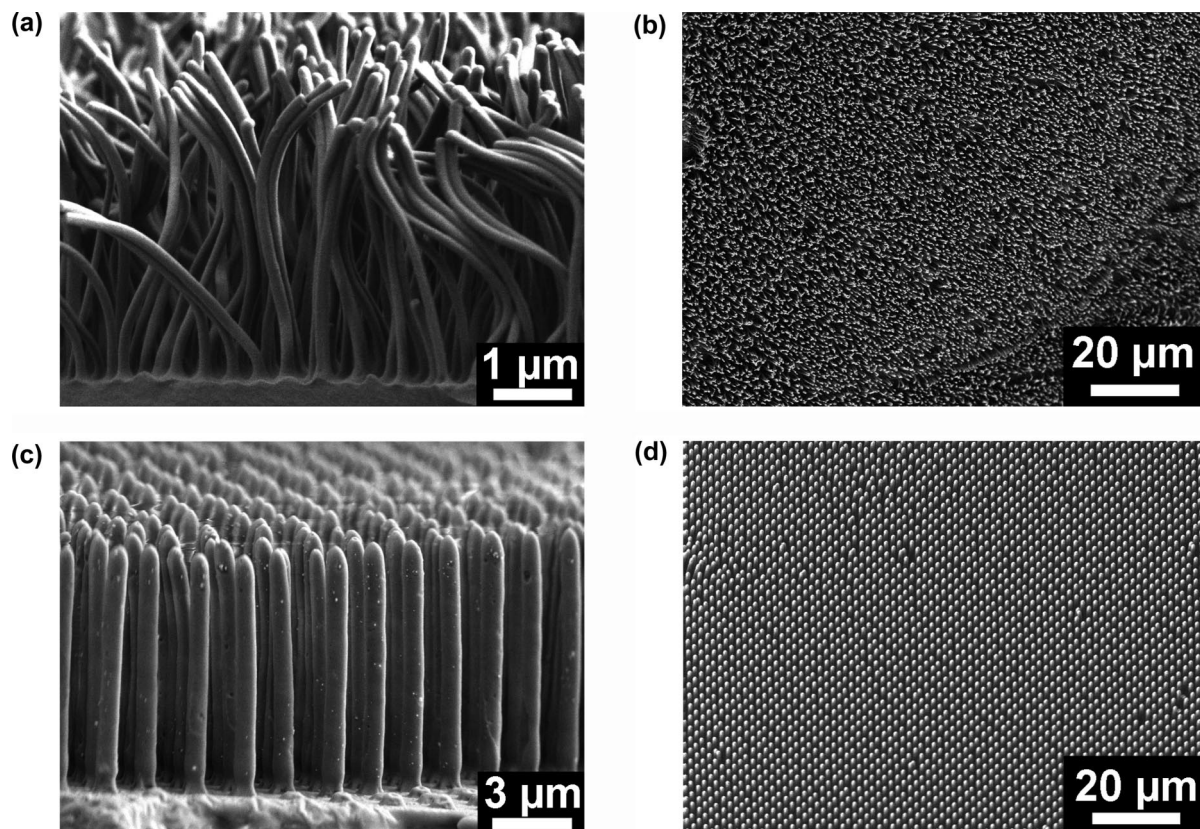


**Figure 3.** SEM images showing arrays of polyacrylate nanofibers and microfibers with aspect ratios of 10 and above. (a) Side view of nanofibers obtained from a 70:30 w/w mixture of PO 77F with tripropylene glycol diacrylate (TPGDA)<sup>36</sup> (cf. Table S1, Supporting Information) with a diameter of  $\approx 120$  nm and an aspect ratio of  $\approx 30$  after their mechanical extraction from an AAO hard template; (b) large-field top view of nanofibers with a diameter of  $\approx 120$  nm and an aspect ratio of  $\approx 30$  after their mechanical extraction from an AAO hard template; (c) side view of microfibers after mechanical extraction from macroporous silicon (pore diameter  $1 \mu\text{m}$ ; pore depth  $10 \mu\text{m}$ ) modified with 1H,1H,2H,2H-perfluorodecyltrichlorosilane; (d) large-field top view of the sample seen in c.

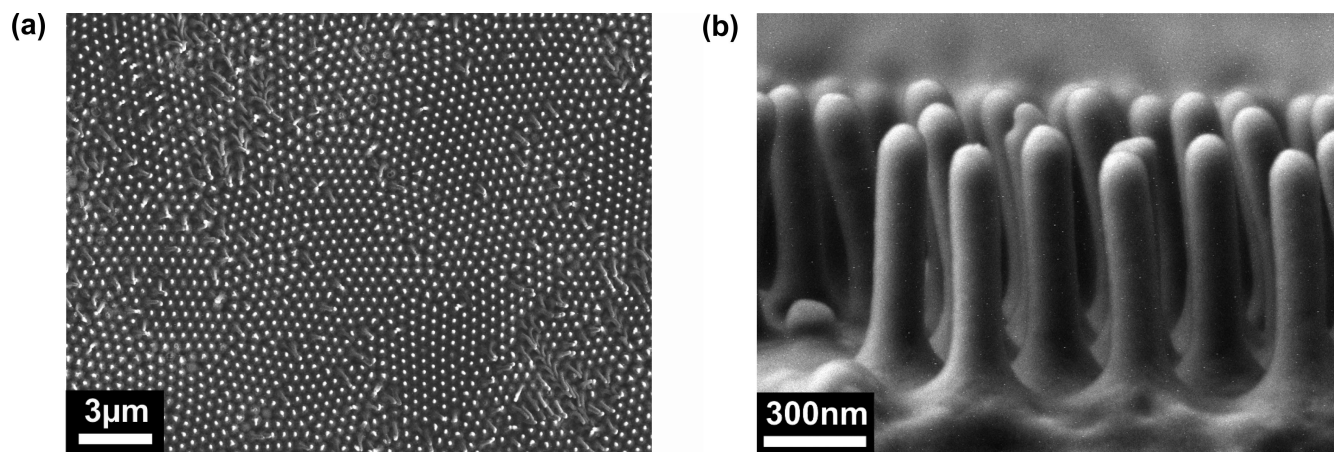


**Figure 4.** SEM images of arrays of polyacrylate nanofibers (diameter  $\approx 120$  nm; length  $\approx 900$  nm) after their use for the preparation of a silica replica and mechanical detachment from the latter. (a) Top view; (b) side view (the nanofibers seen in the SEM image appear to be shorter than they actually are because of the perspective view).

The methodology outlined in Scheme 1 can easily be combined with microstructuring techniques. For example, a thin gold layer was sputtered onto a parent AAO hard template with a pore depth of 900 nm partially covered with a  $500 \mu\text{m}$  thick wire. Before a second sputtering step, the wire was rotated by  $90^\circ$  so that finally an area of about  $500 \mu\text{m} \times 500 \mu\text{m}$  was shadowed. The gold grains deposited onto the surface of the parent AAO hard template served as

seeds for the subsequent electrochemical plating<sup>35</sup> of gold that sealed the pore openings except in the area shadowed during both sputtering steps. In Figure 1a, a large-field view of a polyacrylate nanofiber array obtained after lift-off is shown, which extends correspondingly to about  $500 \mu\text{m} \times 500 \mu\text{m}$ . The top-view image of the same array in Figure 1b reveals that the characteristic domain structure of the parent AAO hard template and the hexagonal order within the

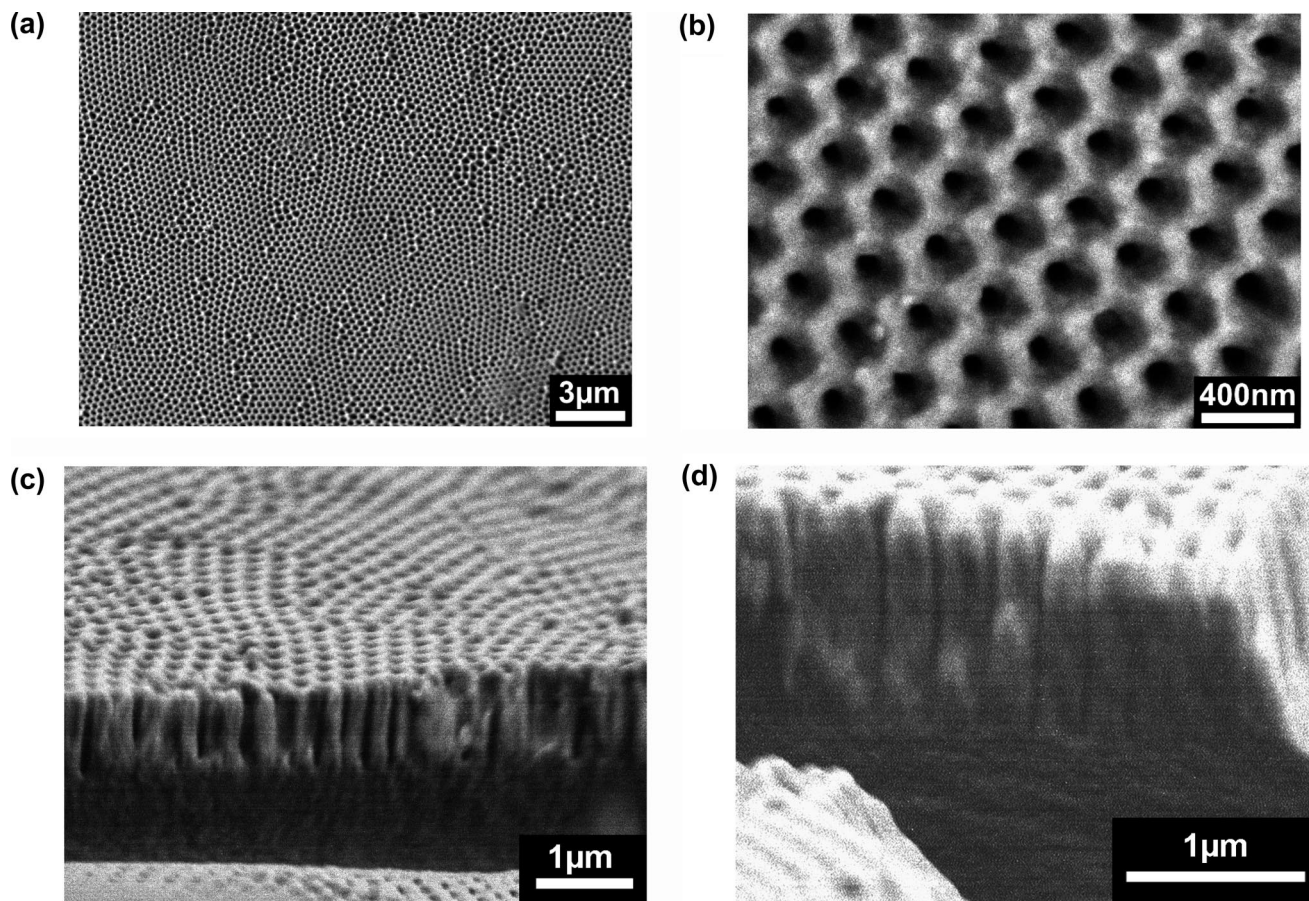


**Figure 5.** SEM images showing the grandchild silica replica of the parent AAO hard templates after heating to 550 °C for 6 h. (a) Large-field top view; (b) top view at higher magnification; (c) large-field side view of a cleaved silica replica; (d) side view at higher magnification.

domains is maintained. The cross-sectional view of the polyacrylate nanofibers in Figure 1c indicates that they do not stick together and stand upright. They possess a uniform diameter and height of about 120 and 900 nm, respectively, corresponding to an aspect ratio (length/diameter) of about 7.5.

In Figure 2a, a large-field view of the parent AAO hard template after the extraction of the polyacrylate nanofiber array is shown. The dark area in the center of the image, which is not covered with gold, is an exact replica of the array shown in Figure 1a, whereas the brighter rim reflects the gold coating. Imaging the surface of the center area at higher magnification reveals that the nanopores are indeed empty (Figure 2b). A cross-sectional view of nanopores located in the center area after extraction of the polyacrylate nanofibers formed in their interior is seen in Figure 2c. The dimensions of the nanopores are in good agreement with those of the extracted nanofibers seen in Figure 1c. It is obvious that the parent AAO hard templates can be recovered after lift-off and are ready for reuse.

It is also possible to detach polyacrylate nanofibers with higher aspect ratios from AAO hard templates possessing accordingly deeper pores. In Figure 3a,b, arrays of polyacrylate nanofibers with a length of 4 μm and a diameter of 120 nm corresponding to an aspect ratio of about 30 are shown. Their careful examination (and a comparison with

the microfibers seen in Figure S1, Supporting Information) revealed that they had a constant diameter along their entire length, suggesting that yielding and necking do not occur upon extraction. However, independent of the way of their release from the hard templates, nanofibers with such high aspect ratios show an intrinsic tendency toward bending and bunching. Bunching is caused by adhesion between adjacent nanofibers and becomes more significant as the potential contact area increases along with their aspect ratio. The use of stiffer materials may allow overcoming these drawbacks but is in turn associated with a stronger tendency toward fracture upon exposure of the nanofibers to mechanical stress, as it is the case during the detachment from the hard templates. However, we anticipate that the lift-off process reported here can be further optimized to produce ordered arrays of free-standing nanofibers (i) by engineering the properties of the material the nanofibers consist of, (ii) by increasing the spacing between the nanopores in the AAO hard templates, for instance, by applying the recently reported hard anodization,<sup>10</sup> and (iii) by optimizing the design of the device configuration used for the mechanical extraction such as to minimize shear. It should be noted that in extended arrays of polyacrylate microfibers with a diameter of 1 μm and a length of 10 μm, which was mechanically detached from macroporous silicon modified with 1H,1H,2H,2H-perfluorodecyltrichlorosilane,<sup>30</sup> neither bending nor bunching

occurred to a significant degree (Figure 3c,d).

To produce silica replicas of parent AAO hard templates with a pore diameter of 120 nm and a pore depth of 900 nm in secondary molding steps, the extracted polyacrylate nanofiber arrays were covered with a TEOS-containing sol as described above. Even after detaching the polyacrylate nanofiber arrays from the gelled silica replicas with a pair of tweezers they remained largely intact, as shown in the large-field view image seen in Figure 4a and the cross-sectional view seen in Figure 4b. Occasionally, adjacent nanofibers stick together. However, it is reasonable to assume that optimization of the material properties and the detachment process will allow multiple uses not only of the parent AAO hard templates but also of the polymeric nanofiber arrays in secondary molding steps.

Figure 5 depicts a nanoporous silica replica after extracting the polyacrylate nanofiber array serving as secondary mold and after subsequent heating to 550 °C for 6 h. The characteristic morphology of the AAO primary molds, which is characterized by domains extending 10 to 20 lattice periods and hexagonal arrangement of the pores within the domains, can be transferred to the nanoporous silica replicas, which withstand high temperatures, as is required for many applications, for example, for their use as catalyst—supports. A representative large-field top view is seen in Figure 5a, and Figure 5b shows openings of the nanopores at higher magnification. The side views of a silica replica seen in Figure 5c,d reveal that the nanopores have a diameter of about 120 nm and a depth of about 900 nm, corresponding to an aspect ratio of 7.5. These values are in reasonable accordance with the dimensions of the polyacrylate nanofibers used as secondary molds.

In conclusion, we have demonstrated the nondestructive mechanical extraction of arrays of polyacrylate nanofibers from thus recyclable AAO hard templates without necking, yielding, fracture, or cohering. The nanofiber arrays were used as secondary molds for the production of nanoporous silica replicas of the parent AAO hard templates. Since the polyacrylate nanofiber arrays were mechanically detached from the nanoporous silica replicas, they can, in principle, also be reused. Nondestructive replication may facilitate high-throughput production of a broad range of ordered nanoporous materials by sol/gel chemistry, electrodeposition, or atomic layer deposition.

**Acknowledgment.** Technical support by S. Kallaus (MPI Halle) as well as by M. Gietl and B. Gossler (University of Bayreuth), funding by the German Research Foundation (Materials World Network, STE 1127/5 and SFB 481, project A6), and the donation of Laromer® resins from BASF SE, Ludwigshafen, is gratefully acknowledged.

**Supporting Information Available:** Properties of the uncured and photo-cross-linked Laromer resins (Table S1); Examples of neck formation upon mechanical extraction of microfibrils (Figure S1). This material is available free of charge via the Internet at <http://pubs.acs.org>.

## References

- (1) Martin, C. R. *Science* **1994**, *266*, 1961.
- (2) Martin, C. R. *Chem. Mater.* **1996**, *8*, 1739.
- (3) Thurn-Albrecht, T.; Schotter, J.; Kastle, G. A.; Emley, N.; Shibauchi, T.; Krusin-Elbaum, L.; Guarini, K.; Black, C. T.; Tuominen, M. T.; Russell, T. P. *Science* **2000**, *290*, 2126.
- (4) Steinhart, M.; Wendorff, J. H.; Greiner, A.; Wehrspohn, R. B.; Nielsch, K.; Schilling, J.; Choi, J.; Gosele, U. *Science* **2002**, *296*, 1997.
- (5) Steinhart, M.; Goring, P.; Dernaika, H.; Prabhakaran, M.; Gosele, U.; Hempel, E.; Thurn-Albrecht, T. *Phys. Rev. Lett.* **2006**, *97*, 027801.
- (6) Masuda, H.; Fukuda, K. *Science* **1995**, *268*, 1466.
- (7) Masuda, H.; Hasegawa, F.; Ono, S. *J. Electrochem. Soc.* **1997**, *144*, L127.
- (8) Masuda, H.; Yada, K.; Osaka, A. *Jpn. J. Appl. Phys. Part 2* **1998**, *37*, L1340.
- (9) Nielsch, K.; Choi, J.; Schwirn, K.; Wehrspohn, R. B.; Gosele, U. *Nano Lett.* **2002**, *2*, 677.
- (10) Lee, W.; Ji, R.; Gosele, U.; Nielsch, K. *Nat. Mater.* **2006**, *5*, 741.
- (11) Arzt, E.; Gorb, S.; Spolenak, R. *Proc. Natl. Acad. Sci. U.S.A.* **2003**, *100*, 10603.
- (12) Lee, H.; Lee, B. P.; Messersmith, P. B. *Nature* **2007**, *448*, 338.
- (13) Geim, A. K.; Dubonos, S. V.; Grigorieva, I. V.; Novoselov, K. S.; Zhukov, A. A.; Shapoval, S. Y. *Nat. Mater.* **2003**, *2*, 461.
- (14) Li, W.-J.; Laurencin, C. T.; Catterton, E. J.; Tuan, R. S.; Ko, F. K. *J. Biomed. Mater. Res.* **2002**, *60*, 613.
- (15) Matthews, J. A.; Wnek, G. E.; Simpson, D. G.; Bowlin, G. L. *Biomacromolecules* **2002**, *3*, 232.
- (16) oner, D.; McCarthy, T. J. *Langmuir* **2000**, *16*, 7777.
- (17) Jin, M.; Feng, X.; Feng, L.; Sun, T.; Zhai, J.; Li, T.; Jiang, L. *Adv. Mater.* **2005**, *17*, 1977.
- (18) Cho, W. K.; Choi, I. S. *Adv. Funct. Mater.* **2008**, *18*, 1089.
- (19) Barthlott, W.; Neinhuis, C. *Planta* **1997**, *202*, 1.
- (20) Yanagishita, T.; Nishio, K.; Masuda, H. *Adv. Mater.* **2005**, *17*, 2241.
- (21) Yanagishita, T.; Nishio, K.; Masuda, H. *Jpn. J. Appl. Phys.* **2006**, *45*, L804.
- (22) Yanagishita, T.; Nishio, K.; Masuda, H. *J. Vac. Sci. Technol. B* **2007**, *25*, L35.
- (23) Park, M.; Harrison, C.; Chaikin, P. M.; Register, R. A.; Adamson, D. H. *Science* **1997**, *276*, 1401.
- (24) Zschech, D.; Kim, D. H.; Milenin, A. P.; Hopfe, S.; Scholz, R.; Goring, P.; Hillebrand, R.; Senz, S.; Hawker, C. J.; Russell, T. P.; Steinhart, M.; Gosele, U. *Nanotechnology* **2006**, *17*, 2122.
- (25) Zschech, D.; Milenin, A. P.; Scholz, R.; Hillebrand, R.; Sun, Y.; Uhlmann, P.; Stamm, M.; Steinhart, M.; Gosele, U. *Macromolecules* **2007**, *40*, 7752.
- (26) Brumlik, C. J.; Martin, C. R. *J. Am. Chem. Soc.* **1991**, *113*, 3174.
- (27) Knez, M.; Nielsch, K.; Niinisto, L. *Adv. Mater.* **2007**, *19*, 3425.
- (28) Lehmann, V. *J. Electrochem. Soc.* **1993**, *140*, 2836.
- (29) Chen, X.; Steinhart, M.; Hess, C.; Gosele, U. *Adv. Mater.* **2006**, *18*, 2153.
- (30) Grimm, S.; Schwirn, K.; Goring, P.; Knoll, H.; Miclea, P. T.; Greiner, A.; Wendorff, J. H.; Wehrspohn, R. B.; Gosele, U.; Steinhart, M. *Small* **2006**, *3*, 993.
- (31) AAO with a pore diameter of 120 nm was prepared following the procedures reported in ref 8. The pores were widened to 200 nm by isotropic etching with a 10 wt % H<sub>3</sub>PO<sub>4</sub> solution at 30 °C for 10 min. After a treatment with aqueous hydrogen peroxide (30%) at 50 °C for 2 h, rinsing with water and drying in air, the AAO was silanized in air for 4 h at 90 °C and then for 4 h at 130 °C in the presence of 0.05 mL of 1H,1H,2H,2H-perfluorodecyltrichlorosilane (C<sub>10</sub>H<sub>4</sub>C<sub>13</sub>-F<sub>17</sub>Si, purchased from ABCR, Karlsruhe, Germany).
- (32) All SEM investigations were performed with a JEOL 7500F scanning electron microscope operated at 3 kV.
- (33) Irgacure 651 (2,2-dimethoxy-1,2-diphenylethane-1-one, CAS No.: 24650–42–8) obtained from Ciba Specialty Chemicals.
- (34) Huber, C. A.; Huber, T. E. *J. Appl. Phys.* **1988**, *64*, 6588.
- (35) We used a commercially available plating solution (Aruna 5000) at a current density of 1 mA/cm<sup>2</sup> and a deposition rate of 0.06 μm/min.
- (36) TPGDA (CAS No.: 42978–66–5) serves as reactive diluent to decrease the viscosity of the resin without reducing network density. To a 70:30 w/w PO 77F/TPGDA mixture 4 wt % of Irgacure 651 (cf. ref 33) was added prior to the infiltration.

NL080842C